

Search and measurement of the SM Higgs boson

S. DONATO ⁽¹⁾ ON BEHALF OF THE ATLAS AND CMS COLLABORATIONS

⁽¹⁾ *University of Zurich, Switzerland*

Summary. — After the success of the LHC Run-1 physics program, the ATLAS and CMS Collaborations have presented their results obtained with the first $\sim 36 \text{ fb}^{-1}$ of integrated luminosity delivered by the LHC at $\sqrt{s} = 13 \text{ TeV}$ in Run-2. We present the main results obtained on the Standard Model Higgs boson, including the searches for specific decay and production channels, and the measurements of the Higgs boson couplings and differential cross section.

PACS: 14.80.Bn Standard-model Higgs bosons

1. – Introduction

The legacy of the LHC Run-1 has been a huge success with the discovery of the standard model (SM) Higgs boson and the first measurement of its properties and couplings. This document summarizes the most important SM Higgs physics results obtained with the ATLAS [1] and CMS [2] experiments using the first $\sim 36 \text{ fb}^{-1}$ of integrated luminosity delivered by the LHC in Run-2 at $\sqrt{s} = 13 \text{ TeV}$.

2. – Observation of $H(\tau\tau)$

The search for the SM Higgs boson decaying into τ leptons performed by the CMS Collaboration in Run-2 data [3] ⁽¹⁾ exploits five final states, depending on the τ lepton decay: $e\mu$, $\mu\tau_h$, $e\tau_h$, $\tau_h\tau_h$, where τ_h refers to the hadronic decay of the τ lepton. The τ_h is identified using a multivariate discriminant, and its energy has been calibrated using $Z \rightarrow \tau_h\tau_h$ events. The same-flavor final states ee and $\mu\mu$ have not been included because of the large Drell-Yan background.

The main background processes are $Z(\tau\tau)$, $W(\ell\nu)+\text{jets}$, $t\bar{t}$, and multijet events. The multijet background is reduced requiring the leptons to be with opposite sign and isolated. The $e\tau_h$ and $\mu\tau_h$ subchannels are contaminated by $W(\ell\nu)+\text{jets}$ events having a jet misidentified as τ_h . In order to reduce this background, the transverse mass of the system

⁽¹⁾ATLAS has recently released a public results on $H(\tau\tau)$ [4].

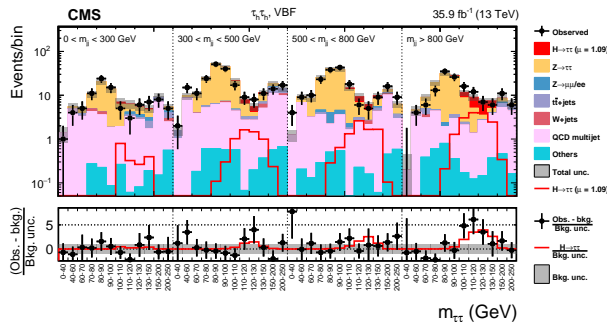


Figure 1. – The 2D fit of the VBF $H \rightarrow \tau_h \tau_h$ category (CMS). The fit is performed using the di-tau ($m_{\tau\tau}$) vs di-jet (m_{jj}) invariant mass distribution [3].

lepton + missing transverse energy is required to be lower than 50 GeV. Fully-leptonic $t\bar{t}$ decay events are rejected in the $e\mu$ category by requiring $p_\zeta - 0.85p_\zeta^{vis} > -35$ or -10 GeV, depending on the category, where p_ζ^{vis} is the missing transverse energy component along the bisector of the two lepton directions, and p_ζ is the total lepton transverse momentum along the same direction.

In order to increase the sensitivity, three categories targeting different production modes have been defined: 0-jet, vector-boson fusion (VBF), and boosted.

Backgrounds are estimated using both simulations and data-driven methods. The $Z(\tau\tau)$ background is taken from simulation after having applied corrections based on $Z(\mu\mu)$ data. Simulations are also used to estimate the $t\bar{t}$ and $W(\ell\nu)$ +jets backgrounds, while their normalizations are extracted from two control regions defined by inverting, respectively, the transverse mass and p_ζ cuts. The multijet background is entirely estimated from data inverting the lepton isolation cut and requiring a same-sign charge.

The invariant mass of the τ pair ($m_{\tau\tau}$) is the most powerful variable to separate $Z(\tau\tau)$ from $H(\tau\tau)$. However, the visible ditau invariant mass is largely overlapping between the Z and Higgs boson masses because of the presence of neutrinos from the τ decay. The SVFIT algorithm [5] has been adopted in the attempt to measure the whole $m_{\tau\tau}$ mass assuming the most-likely kinematic properties of the neutrinos in the event.

The signal is extracted using either a 1D or 2D fit of the most discriminating variables. For example, Fig. 1 shows the 2D fit in the VBF $\tau_h \tau_h$ channel.

The fitted signal strength is $\mu = \frac{\sigma}{\sigma_{SM}} = 1.09_{-0.15}^{+0.15}(\text{stat})_{-0.15}^{+0.16}(\text{syst})_{-0.08}^{+0.10}(\text{theo})_{-0.12}^{+0.13}(\text{bkg stat})$, corresponding to a significance of 4.9σ observed (4.7σ expected). Combining this result with the CMS measurement at 8 TeV, the signal strength is $\mu = 0.98 \pm 0.18$, corresponding to an observed and expected significance of 5.9σ . This is the first observation of $H \rightarrow \tau\tau$ obtained by a single experiment.

3. – Evidence of $t\bar{t}H$

3.1. $t\bar{t}H$ in multilepton final states. – In the $t\bar{t}H$ production channel ⁽²⁾, the Higgs boson is produced in association with a top quark pair. The Higgs boson can decay into

⁽²⁾The $t\bar{t}H$ production has been observed by CMS using 2015-16 data [6] and later by ATLAS including also 2017 data [7].

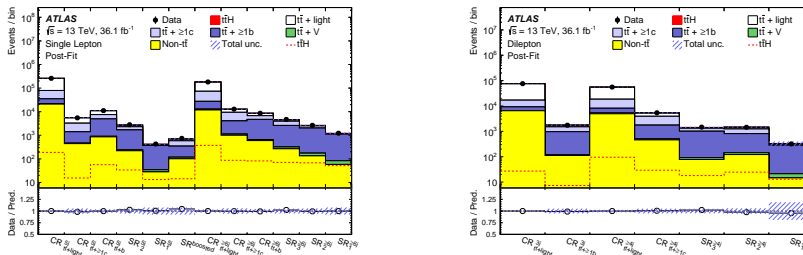


Figure 3. – Analysis categories of the search for $ttH(bb)$ performed by the ATLAS Collaboration in the semi-leptonic (left) and fully-leptonic (right) top-quark decay [10].

the b-tagging discriminator value of jets, forming 9 signal regions with different purities and 10 control regions, useful to constrain the normalization of the backgrounds. The analysis categories definition together with their signal and background composition are shown in Fig. 3. The signal is extracted fitting simultaneously in all signal and control regions a multivariate discriminator to increase the signal/background separation. The results obtained by the ATLAS Collaboration in the search for $H \rightarrow bb$, together with the other ttH searches and their combination, are shown in Tab. II. This is the first evidence for ttH production obtained by a single experiment.

TABLE II. – Results of all Run-2 ttH searches performed by the ATLAS Collaboration and their combination [8].

Channel	Obs. best-fit μ	Exp. best-fit μ	Obs. significance	Exp. significance
Multilepton	$1.6^{+0.5}_{-0.4}$	$1.0^{+0.4}_{-0.4}$	4.1σ	2.8σ
$H \rightarrow bb$	$0.8^{+0.6}_{-0.6}$	$1.0^{+0.6}_{-0.6}$	1.4σ	1.6σ
$H \rightarrow \gamma\gamma$	$0.6^{+0.7}_{-0.6}$	$1.0^{+0.8}_{-0.6}$	0.9σ	1.7σ
$H \rightarrow 4\ell$	< 1.9	$1.0^{+3.2}_{-1.0}$	—	0.6σ
Combined	$1.2^{+0.3}_{-0.3}$	$1.0^{+0.3}_{-0.3}$	4.2σ	3.8σ

4. – Evidence of $VH(bb)$

The most sensitive channel to search for the $H \rightarrow bb$ is the associated production of the Higgs boson with a vector boson decaying into leptons (VH). The leptonic decay of the vector boson is useful to reject the large multijet production from strong interactions. The analyses performed by the ATLAS and CMS collaborations are described, respectively, in Refs. [13] and [14].

The most discriminating variables between signal and background are the di-jet invariant mass and the b-tagging values of jets. In order to improve the di-jet invariant mass resolution, a special calibration for b jets is adopted. This calibration is obtained exploiting several variables, including those related to the possible presence of a soft lepton originated from the B hadron decay. A way to further improve the di-jet invariant mass resolution is the kinematic fit, where $Z(\ell\ell)H(bb)$ candidate events are constrained to have no missing transverse energy. The analysis is subdivided into categories depending

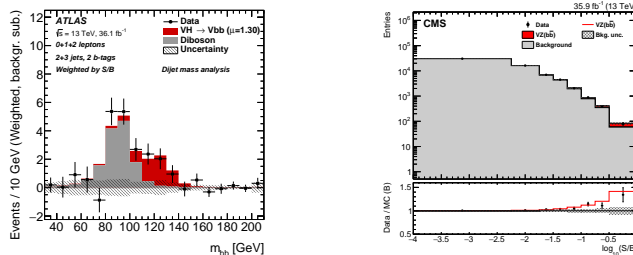


Figure 4. – Dijet mass distribution after the subtraction of all expected backgrounds (ATLAS, left) and combination of all signal region plots merging bins having the same purity (CMS, right) [14].

on the number of leptons, jets, b-tagged jets, and on the momentum of the vector boson candidate. The main backgrounds are $Z/W + \text{jets}$ and $t\bar{t}$. Backgrounds are estimated using simulations, but their normalizations are free parameters of the fit. In order to constrain the background normalizations, dedicated control regions enriched with each of the backgrounds are included in the fit. The final fit is performed by fitting simultaneously all signal and control regions. The distribution of a multivariate discriminant is fitted in signal regions in order to increase the separation between signal and background.

As an analysis cross-check, the $VZ(bb)$ process has been measured using a similar analysis strategy. The measurement obtained by ATLAS is $\mu_{Z(bb)} = 1.11 \pm 0.23$ and by CMS is 1.02 ± 0.22 , both of which are compatible with SM predictions. The result for the $VH(bb)$ searches is $\mu = 0.90 \pm 0.18(\text{stat})_{-0.19}^{+0.21}(\text{syst})$ by ATLAS, corresponding to an excess of 3.6σ (4.0σ expected) over the background. The signal strength measured by CMS is $\mu = 1.06_{-0.29}^{+0.31}$, corresponding to an excess of 3.8σ (3.8σ expected). Figure 4 shows respectively the di-jet mass distribution after the subtraction of all expected backgrounds except VV and the combination of all signal region histograms merging bins having the same purity.

5. – Other Higgs boson searches

5.1. Search for $VH(cc)$. – The $VH(cc)$ search is similar to $VH(bb)$ but it looks for the decay of the Higgs boson into charm quarks. It has been performed by ATLAS in 2016 data [15] in the two lepton final state and exploiting a charm-jet tagger recently developed [16]. This tagger has been calibrated using $W \rightarrow cs/cd$ decay data. The challenges of this channel are the small branching fraction $H \rightarrow cc$ ($\sim 2.9\%$), the difficulty to tag charm jets, the large $Z(\ell\ell) + c\text{-jets}$ background, the $H \rightarrow bb$ background peaking at the same mass of the signal $H \rightarrow cc$. A validation analysis has been performed looking for $ZW(cs)$ and $ZZ(cc)$. The result is $\mu_{VV} = 0.4_{-0.4}^{+0.5}$, corresponding to a significance of 1.4σ (2.2σ expected). The result for the search for $VH(cc)$ is $\mu = -69 \pm 101$ with a 95% confidence level (CL_s) upper limit of $\mu < 100$ ($\mu < 150$ expected).

5.2. Search for boosted $H(bb)$. – An inclusive search for boosted $H \rightarrow bb$ with $p_T > 450$ GeV has been performed by the CMS Collaboration [17]. This analysis reconstructs the Higgs boson as a wide jet with $\Delta R = 0.8$ and exploits substructure techniques to reconstruct the two subjets, to reduce the pile-up effects, and to improve the mass resolution. A specific double b-tagger has been developed for this analysis to identify wide

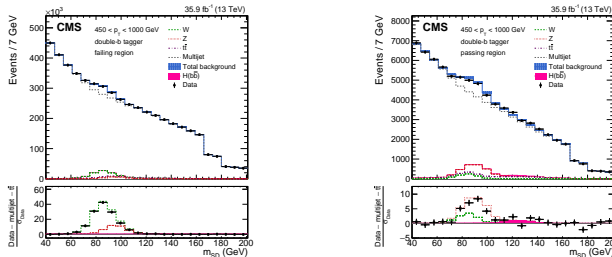


Figure 5. – Wide-jet mass distribution for the antitag (left) and double b tag (right) regions in the search for boosted $H(bb)$ with the CMS experiment [17].

jets containing two B hadrons like $H \rightarrow bb$ [18]. The main backgrounds are multijets, Z+jets, and W+jets events. The multijet background has been estimated inverting b tagging and applying a transfer function obtained from sidebands, as shown in Fig. 5, where the W/Z peak is clearly visible. The best-fit signal strength is $\mu = 2.3 \pm 1.5(\text{stat})_{-0.4}^{+1.0}(\text{syst})$, corresponding to a significance of 1.5σ (0.7σ expected).

5.3. Search for $H(Z\gamma)$. – The $H \rightarrow Z\gamma$ is a further Higgs boson decay that will be accessible at the LHC. In the analysis performed by ATLAS [19] ⁽⁴⁾, the $Z\gamma$ peak is searched over a smoothly falling background in the invariant mass spectrum. The Z boson is reconstructed in the dimuon and dielectron decay. The analysis is divided in different categories targeting different production channels. In particular, the vector boson fusion category has the largest sensitivity. The final result is a 95% CL_s upper limit on the cross section of 6.6 times the SM Higgs boson prediction (5.2 expected).

5.4. Search for $H(\mu\mu)$. – The branching fraction of the SM Higgs boson decay into muons is very small ($\sim 2 \cdot 10^{-4}$). This channel is the most sensitive way to probe the Higgs boson coupling with second-generation particles. Despite the small branching fraction, ATLAS and CMS aim to observe this process in the next years exploiting the large integrated luminosity expected to be delivered by the LHC. The Run-2 ATLAS and CMS analyses [21, 22] reached large improvements in sensitivity compared to those from Run-1. The searches have been performed looking for the peak in the dimuon invariant mass distribution over a falling smoothly background. The sensitivity has been enhanced splitting the phase space in categories with different purities, using a multivariate discriminant. Figure 6 shows the distribution of such multivariate discriminant distribution and the dimuon mass spectrum obtained after having combined all categories reweighted according to their purity. The results are $\mu = 0.9_{-0.9}^{+1.0}$, corresponding to an observed (expected) significance of 0.98σ (1.09σ), for CMS and $\mu = -0.1 \pm 1.4$ for ATLAS.

5.5. Search for $H(\text{light quarks})$. – The search of the Higgs boson decaying to light quarks has been performed by ATLAS collaboration looking for the $H \rightarrow \phi\gamma$ and $H \rightarrow \rho(770)\gamma$ decays [23]. The final state considered requires two isolated tracks with $p_T > 35$ GeV with an invariant mass compatible with ρ or ϕ and one photon with $p_T > 15$ GeV. The background is estimated using a data-driven technique, and it has been validated exploiting ρ and ϕ sidebands. The 95% CL_s upper limit on the branching ratio found are

⁽⁴⁾The recent CMS results are in Ref. [20].

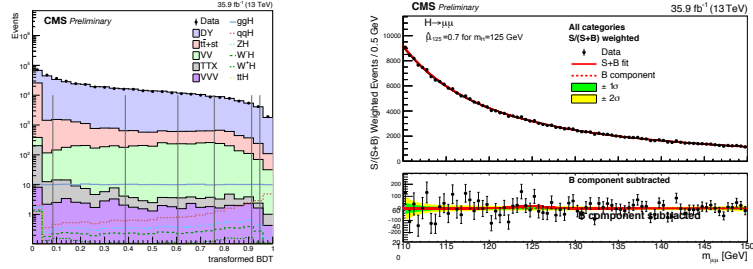


Figure 6. – Multivariate discriminant distribution defining $H \rightarrow \mu\mu$ categories (left) and dimuon mass distribution (right) obtained by the CMS Collaboration [22].

$4.8 \cdot 10^{-4}$ ($4.2 \cdot 10^{-4}$ expected) for $H(\phi\gamma)$ and $8.8 \cdot 10^{-4}$ ($8.4 \cdot 10^{-4}$ expected) for $H(\rho\gamma)$. These limits correspond to $\mu < 208$ (182 expected) for $H(\phi\gamma)$ and $\mu < 52$ (50 expected) for $H(\rho\gamma)$.

6. – Precision Higgs boson measurements

6.1. Differential cross section. – The Higgs boson decays to photons ($H \rightarrow \gamma\gamma$) and to four leptons ($H \rightarrow 4\ell$) are the most sensitive channels to provide precision measurements of the Higgs boson. The Run-2 measurements of the Higgs boson cross section obtained by ATLAS and CMS as a function of the centre-of-mass energy are shown in Fig. 7 [24, 25, 26]⁽⁵⁾. The growing signal allows to measure the differential cross section as a function of variables like the Higgs boson p_T and η . Fig. 8 shows the fiducial $H \rightarrow \gamma\gamma$ cross section as a function of the Higgs boson p_T . The 13-TeV $H \rightarrow 4\ell$ and $H \rightarrow \gamma\gamma$ analyses have been also used to measure Higgs boson couplings with fundamental particles, including the effective loop-induced coupling with gluons and photons. All results obtained so far are compatible with the SM expectations. Fig. 9 shows the 2D measurement of the coupling modifier for fermions (κ_f) and vector bosons (κ_V). The sensitivities of these analyses are already close to that of the Run-1 ATLAS+CMS

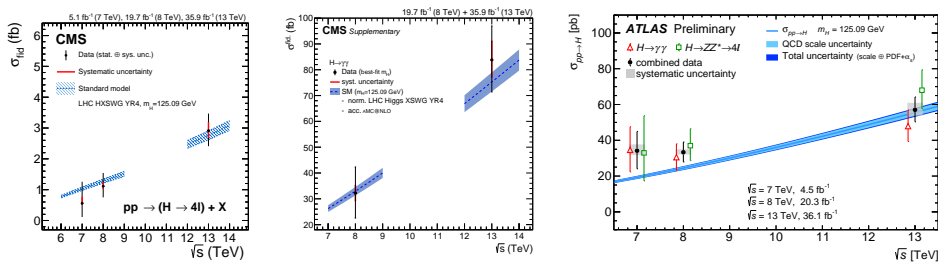


Figure 7. – Higgs boson cross section as a function of the centre-of-mass energy for $H \rightarrow 4\ell$ (left) and $H \rightarrow \gamma\gamma$ (center) channels measured by CMS, and both channels with their combination measured by ATLAS (right) [24, 25, 26].

⁽⁵⁾A recent combination of the Run-2 CMS Higgs boson analyses with the measurements of couplings and signal strengths is available in Ref. [28]

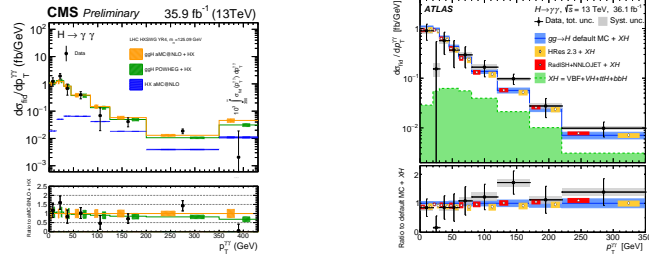


Figure 8. – Higgs boson cross section as a function of the Higgs boson p_T as measured in the $H \rightarrow \gamma\gamma$ channel by CMS (left) [27] and ATLAS (right) [24].

combination paper [29].

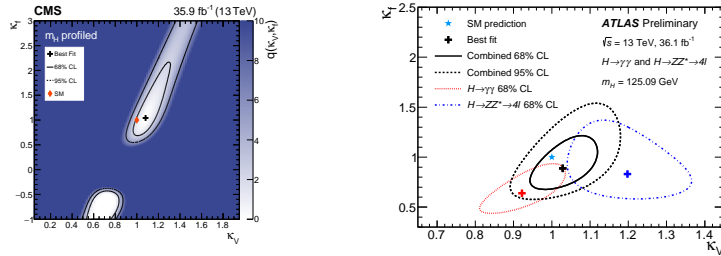


Figure 9. – Higgs boson coupling modifier of fermions (κ_f) and vector bosons (κ_V) as measured by ATLAS (left) and CMS (right). The ATLAS plot is obtained using both $H \rightarrow 4\ell$ and $H \rightarrow \gamma\gamma$ data, while the CMS result includes only $H \rightarrow \gamma\gamma$ [29, 30].

7. – Conclusions

The ATLAS and CMS collaborations published many important Higgs results in the last year, including the single-experiment observation of $H \rightarrow \tau\tau$, the evidence for $H \rightarrow bb$ and ttH production, brand new Higgs boson searches (e.g. boosted $H \rightarrow bb$, $H \rightarrow cc$), and a large improvement on the search for $H \rightarrow \mu\mu$. The $H \rightarrow 4\ell$ and $H \rightarrow \gamma\gamma$ channels are used to measure differential cross sections and couplings. All results shown have been obtained using the first $\sim 36 \text{ fb}^{-1}$ collected in LHC Run-2. In 2017, the LHC doubled the integrated luminosity, and even more data are expected to be collected in 2018. Many more results are expected to be published in the next months.

REFERENCES

- [1] G. Aad *et al.* [ATLAS Collaboration], JINST **3** (2008) S08003. doi:10.1088/1748-0221/3/08/S08003
- [2] S. Chatrchyan *et al.* [CMS Collaboration], JINST **3** (2008) S08004. doi:10.1088/1748-0221/3/08/S08004
- [3] A. M. Sirunyan *et al.* [CMS Collaboration], Phys. Lett. B **779** (2018) 283 doi:10.1016/j.physletb.2018.02.004 [arXiv:1708.00373 [hep-ex]].
- [4] ATLAS collaboration, ATLAS-CONF-2018-021.

- [5] L. Bianchini, J. Conway, E. K. Friis and C. Veelken, *J. Phys. Conf. Ser.* **513** (2014) 022035. doi:10.1088/1742-6596/513/2/022035
- [6] A. M. Sirunyan *et al.* [CMS Collaboration], *Phys. Rev. Lett.* **120** (2018) no.23, 231801 doi:10.1103/PhysRevLett.120.231801, 10.1130/PhysRevLett.120.231801 [arXiv:1804.02610 [hep-ex]].
- [7] M. Aaboud *et al.* [ATLAS Collaboration], arXiv:1806.00425 [hep-ex].
- [8] M. Aaboud *et al.* [ATLAS Collaboration], *Phys. Rev. D* **97** (2018) no.7, 072003 doi:10.1103/PhysRevD.97.072003 [arXiv:1712.08891 [hep-ex]].
- [9] A. M. Sirunyan *et al.* [CMS Collaboration], arXiv:1803.05485 [hep-ex].
- [10] M. Aaboud *et al.* [ATLAS Collaboration], *Phys. Rev. D* **97** (2018) no.7, 072016 doi:10.1103/PhysRevD.97.072016 [arXiv:1712.08895 [hep-ex]].
- [11] A. M. Sirunyan *et al.* [CMS Collaboration], arXiv:1803.06986 [hep-ex].
- [12] A. M. Sirunyan *et al.* [CMS Collaboration], arXiv:1804.03682 [hep-ex].
- [13] M. Aaboud *et al.* [ATLAS Collaboration], *JHEP* **1712** (2017) 024 doi:10.1007/JHEP12(2017)024 [arXiv:1708.03299 [hep-ex]].
- [14] A. M. Sirunyan *et al.* [CMS Collaboration], *Phys. Lett. B* **780** (2018) 501 doi:10.1016/j.physletb.2018.02.050 [arXiv:1709.07497 [hep-ex]].
- [15] M. Aaboud *et al.* [ATLAS Collaboration], *Phys. Rev. Lett.* **120** (2018) no.21, 211802 doi:10.1103/PhysRevLett.120.211802 [arXiv:1802.04329 [hep-ex]].
- [16] ATLAS Collaboration [ATLAS Collaboration], ATLAS-PHYS-PUB-2017-013.
- [17] A. M. Sirunyan *et al.* [CMS Collaboration], *Phys. Rev. Lett.* **120** (2018) no.7, 071802 doi:10.1103/PhysRevLett.120.071802 [arXiv:1709.05543 [hep-ex]].
- [18] A. M. Sirunyan *et al.* [CMS Collaboration], *JINST* **13** (2018) no.05, P05011 doi:10.1088/1748-0221/13/05/P05011 [arXiv:1712.07158 [physics.ins-det]].
- [19] M. Aaboud *et al.* [ATLAS Collaboration], *JHEP* **1710** (2017) 112 doi:10.1007/JHEP10(2017)112 [arXiv:1708.00212 [hep-ex]].
- [20] CMS Collaboration, CMS-PAS-HIG-17-007, <https://cds.cern.ch/record/2256103>.
- [21] M. Aaboud *et al.* [ATLAS Collaboration], *Phys. Rev. Lett.* **119** (2017) no.5, 051802 doi:10.1103/PhysRevLett.119.051802 [arXiv:1705.04582 [hep-ex]].
- [22] CMS Collaboration, CMS-PAS-HIG-17-019, <https://cds.cern.ch/record/2292159>.
- [23] M. Aaboud *et al.* [ATLAS Collaboration], arXiv:1712.02758 [hep-ex].
- [24] ATLAS collaboration, ATLAS-CONF-2017-047, <https://cds.cern.ch/record/2273854>.
- [25] A. M. Sirunyan *et al.* [CMS Collaboration], *JHEP* **1711** (2017) 047 doi:10.1007/JHEP11(2017)047 [arXiv:1706.09936 [hep-ex]].
- [26] CMS Collaboration, CMS-PAS-HIG-17-015, <https://cds.cern.ch/record/2257530>.
- [27] A. M. Sirunyan *et al.* [CMS Collaboration], arXiv:1804.02716 [hep-ex].
- [28] CMS Collaboration, CMS-PAS-HIG-17-031, <https://cds.cern.ch/record/2308127>.
- [29] G. Aad *et al.* [ATLAS and CMS Collaborations], *JHEP* **1608** (2016) 045 doi:10.1007/JHEP08(2016)045 [arXiv:1606.02266 [hep-ex]].
- [30] M. Aaboud *et al.* [ATLAS Collaboration], arXiv:1802.04146 [hep-ex].